Laser and Particle Beams (2014), *32*, 79–88.
© Cambridge University Press, 2013 0263-0346/13 $20.00
doi:10.1017/S0263034613000803

Collisional effects on the relativistic current-filamentation instability in dense plasmas

B. HAO,[1] Z.M. SHENG,[2] J. ZHANG,[1,2] AND Y.T. LI[1]

[1]Beijing National Laboratory of Condensed Matter Physics, Institute of Physics, Chinese Academy of Sciences, Beijing, China
[2]Key Laboratory for Laser Plasmas (Ministry of Education) and Department of Physics and Astronomy, Shanghai Jiao Tong University, Shanghai, China

(Received 28 June 2013; Accepted 21 August 2013)

Abstract

Collisional effects on the current-filamentation instability (CFI), accounting for the space charge effect (SCE), are investigated kinetically for a relativistic beam propagating in dense plasmas. It is shown that collisions can completely suppress the SCE in low temperature dense plasma, leading to enhancement of the CFI. This kind of decoupling mechanism is quite different from the well-known resistive mechanism [Molvig (1975). *Phys. Rev. Lett.* 35, 1504]. In particular, we find the present decoupling mechanism can well explain the recent numerical simulation results [Karmakar *et al.* (2008). *Phys. Rev. Lett*. doi: 101, 255001]. In the parameter regime related to the laser-solid interaction and fast ignition scenario (FIS), the CFI growth rate with SCE included is enhanced in the low plasma density region through the decoupling mechanism. In the high plasma density region, it is enhanced mainly through the resistive mechanism.

Keywords: Collisional effect; Dense plasma; Filamentation instability; Relativistic electron beam

1. INTRODUCTION

The electromagnetic instability in a beam-plasma system, often called Weibel instability or current-filamentation instability (CFI), is a well-known phenomenon (Weibel, 1959) and has been studied extensively for its linear and nonlinear development under various parameter conditions (Molvig, 1975; Lee & Thode, 1983; Pegoraro *et al.*, 1996; Califano *et al.,* 1998, Honda *et al.*, 2000; Bret *et al.*, 2005; Kong *et al.*, 2009; Stockem *et al.*, 2009; Mondal *et al.*, 2012; Hao *et al.*, 2012). Not only in laboratory plasmas, such instabilities are also supposed to develop in astrophysical environments (Medvedev *et al.*, 1999; Fonseca & Silva, 2003; Takabe *et al.*, 2008). In the last decade, the problem of electron beam transport in dense plasma has received tremendous interest because it is closely related to the fast ignition scenario (FIS) of laser inertial confinement fusion (Tabak *et al.*, 1994; Kodama *et al.*, 2001), as well as to particle acceleration and radiation sources from relativistic laser-solid interactions (Tatarakis *et al.*, 2003; Roth *et al.*, 2005; Baton *et al.*, 2005; Duclousa *et al.*, 2008; Jung *et al.*, 2009; Storm *et al.*, 2009; Zhou *et al.*, 2012; Lalousis *et al.*, 2012; Lin *et al.*, 2012; Li *et al.*, 2012). In the FIS, it is required that an extremely large flux relativistic beam penetrates a relatively cold and dense plasma with the density ranging from 10^{21}cm^{-3} to 10^{26}cm^{-3}, and deposits its energy in the core (Bell *et al.*, 1997; Meyer-ter-Vehn *et al.*, 2005; Chrisman *et al.*, 2008). Propagating of such a large flux of current in the background plasma will naturally result in CFI, two-stream instability, the oblique instability, and anisotropydriven instability (Bludman *et al.*, 1960; Startsev *et al.*, 2002; Bret *et al.*, 2008; Hao *et al.*, 2012).

In the presence of dense background plasma concerned with FIS, special attention has been paid to the collisional effects on CFI (Gremillet *et al.*, 2002; Honda, 2004; Hill *et al.*, 2005; Bret *et al.*, 2006; 2009; Cottrill *et al.*, 2008; Karmakar *et al.*, 2008; Hao *et al.*, 2009; Bret, 2010; Deutsch & Didelez, 2011; Sakagami *et al.*, 2012). Although the pure CFI (without longitudinal perturbation) may not be the fastest growing mode in the collisionless case, it can be the fastest one in the collisional case (Hao *et al.*, 2012). Furthermore, it is considered to be responsible for the strong quasi-static magnetic fields (Pukhov *et al.*, 1997; Medvedev *et al.*, 1999; Sentoku *et al.*, 2000), which is significantly important for the transport and energy deposition of the relativistic electron beam (Honda *et al.*, 2000; Sentoku *et al.*, 2003; Honrubia & Meyer-ter-Vehn, 2008). Since the fusion target is dense

Address correspondence and reprint request to: Z.M. Sheng, Key Laboratory for Laser Plasmas (Ministry of Education) and Department of Physics and Astronomy, Shanghai Jiao Tong University, Shanghai, China. E-mail: zmsheng@sjtu.edu.cn

https://doi.org/10.1017/S0263034613000803 Published online by Cambridge University Press

and cold, collisions between the background plasma particles will obviously alter the CFI. The transition from collisionless filamentation, generating small scale filaments, to resistive filamentation with large scale filaments has been discussed (Bret *et al.*, 2009; Bret, 2010).

The investigations of the collisional effects on the CFI used to focus on the resistive mechanism (Molvig, 1975; Okada & Niu, 1980; Hao *et al.*, 2008), where the combination of the collision and thermal spread on the CFI is concerned. And it is generally shown in a two-dimensional kinetic theory that collision in fact plays dual roles (Hao *et al.*, 2008; 2009*a*). On one hand, the collision resistive force parallel to the perturbation wave vector causes detuning between the particle density perturbations and the reactive fields, which attenuates the CFI. On the other hand, the collision resistive force perpendicular to the perturbation wave vector interferes with the background plasma collective motion and cancels the stabilization effect of the dense plasma, which enhances the CFI. At last, their combination tends to attenuate the CFI for a symmetric (where the background electron density equals the beam density) or quasi-symmetric counter-streaming system, and enhance the CFI for an extremely asymmetric (where the background electron density is much higher than the beam density) counter-streaming system. However, these studies have either ignored the space charge effect (SCE) (Tzoufras *et al.*, 2006; Hao *et al.*, 2009*a*), or limited to the nonrelativistic case (Hao *et al.*, 2008), or limited to collisionless plasma (Bret, 2007). As we have shown kinetically (Hao *et al.*, 2009*b*), the CFI of a hot-beam warm-plasma system in fact could be mainly suppressed by the SCE in addition to the thermal spread (Silva *et al.*, 2002). Therefore, the CFI cannot be enhanced if collisions cannot interfere with the SCE.

In the present work, we extend our previous relativistic studies to include the SCE, which helps one to get a complete understanding of the collisional effects on the CFI. In order to compare with the simulation results based on the fluid model (Karmakar *et al.*, 2008), we also present the numerical results obtained from the water-bag distribution for beam and plasma electrons. Our results show that collisional effects can destroy the coupling between the CFI and the ion acoustic mode, leading to the suppression of the SCE if the collision frequency is large enough. Therefore, the CFI can be increased by collision through such kind of decoupling mechanism even for symmetric or quasi-symmetric counter streaming. Moreover, it is found that the collisional CFI may not necessary be the instability of the unstable negative-energy magneto sound waves driven by collisions in the background plasma as claimed in the previous study (Karmakar *et al.*, 2008). Instead, the enhanced CFI may be due to the attenuation of the SCE due to collision.

The paper is organized as follows. In Section 2, the basic theory for the linear collisional dispersion relation is presented. In Section 2, the collisional dispersion equation is solved numerically. For comparison, the results under water-bag distribution is also given. The involved physical mechanisms are argued in details. Then, the present theory is applied to the parameter regime related to the FIS and laser-solid interactions. Finally, we conclude with a summary in Section 4.

2. KINETIC DISPERSION RELATION

The plasma is assumed to be homogeneous and unmagnetized, where the ions are deuterium or tritium immobile to form a charge neutralized background. The system is described by the Vlasov-Krook-Maxwell equations (Bhatnagar *et al.*, 1954; Lee & Thode, 1983)

$$\frac{\partial f_\alpha}{\partial t}+\vec{v}_\alpha\cdot\frac{\partial f_\alpha}{\partial \vec{r}}+q_\alpha\left(\vec{E}+\frac{\vec{v}_\alpha\times\vec{B}}{c}\right)\cdot\frac{\partial f_\alpha}{\partial \vec{p}_\alpha} = \nu_\alpha\left(f_{0\alpha}-f_\alpha+f_{0\alpha}\frac{\delta n_\alpha}{n_{0\alpha}}\right), \tag{1}$$

$$\nabla\times\vec{B}=\frac{1}{c}\frac{\partial\vec{E}}{\partial t}+\frac{4\pi}{c}\sum_\alpha\vec{j}_\alpha, \tag{2}$$

$$\nabla\times\vec{E}=-\frac{1}{c}\frac{\partial\vec{B}}{\partial t}, \tag{3}$$

where $\alpha = b, p$ labels the beam electrons and the background electrons, respectively, $\delta n_\alpha=\int(f_a-f_{0\alpha})d\vec{p}_\alpha$, $\vec{j}_\alpha=q_\alpha\int f_\alpha\vec{v}_\alpha d\vec{p}_\alpha$, $q_\alpha n_\alpha, \nu_\alpha, f_{0\alpha}$, and c correspond to the electron charge, the electron density, the effective collision frequency, the local equilibrium distribution function, and the light speed in vacuum, respectively, $n_{0\alpha}$ is the unperturbed electron density. Although the Krook model (Bhatnagar *et al.*, 1954) does not conserve the momentum and energy of the electrons, we still use it here since the electrons will lose energy to the plasma ions at the initial stage of FIS. Since ν_b is usually much smaller than the CFI growth rate (Hao *et al.*, 2009*a*), we neglect it here. The background electron collision frequency is treated in the way as we did in previous work (Hao *et al.*, 2009*a*). But here Krook collisional term on the right-hand side of Eq. (1) is written in a way that the particle number is conserved.

We assume the beam drifts along the e_z direction and the perturbation wave vector is in the direction e_x, with the electromagnetic components $E_{EM}=E_z e_z$ and $B_{EM}=B_y e_y$, and the electrostatic component $E_{ES}=\mathrm{E}_x e_x$. Usually one assumes that the return current from plasma electrons can well compensate the beam current. As argued by Breizman *et al.* (1974 and references therein), the current compensation condition takes the form

$$\sigma\gg\frac{\tau}{4\pi}\frac{c^2}{r_b^2}, \tag{4}$$

where the conductivity $\sigma=\omega_p^2/[4\pi(\nu_p+1/\tau)]$, τ is the beam electron duration, and r_b is the beam radius. For the cone guided FIS (Kodama *et al.*, 2001), $\tau\sim 10$ ps, $r_b\sim 20\,\mu$m,

https://doi.org/10.1017/S0263034613000803 Published online by Cambridge University Press

and the background electron density n_p is $10^{23} \sim 10^{26}\mathrm{cm}^{-3}$. It can be obtained that $4\pi\sigma r_b^2/\tau c^2 > 100$. Thus, the beam current can be well compensated by the plasma electrons and the initial magnetic field can be assumed to be zero. Now linearizing Eqs. (1)–(3) by assuming the perturbations are in the form of $\exp[i(\vec{k}\cdot\vec{r}-\omega t)]$ with $\vec{k}=k\hat{e}_x$ for pure CFI, we can get the well-established linearized kinetic dispersion relation

$$(\varepsilon_{zz}-k^2c^2/\omega^2)\varepsilon_{xx}=\varepsilon_{xz}\varepsilon_{zx}, \tag{5}$$

where the dielectric tensor is

$$\begin{aligned}\varepsilon_{ij}=\delta_{ij}&+\frac{\omega_b^2}{n_{0b}\omega^2}\left[\int\frac{p_{bi}}{\gamma_b^*}\frac{\partial f_{0b}}{\partial p_{bj}}d\vec{p}_b+\int\frac{p_{bi}p_{bj}}{\gamma_b^*}\frac{\vec{k}\cdot\partial f_{0b}/\partial\vec{p}_b}{m\gamma_b^*\omega-\vec{k}\cdot\vec{p}_b}d\vec{p}_p\right]\\&+\frac{\omega_p^2}{n_{0b}\omega^2}\left[\int\frac{p_{pi}(m\omega-\vec{k}\cdot\vec{p}_p)}{m\Omega}\frac{\partial f_{0p}}{\partial p_{pj}}d\vec{p}_p+\int\frac{p_{pi}p_{pj}\vec{k}\cdot\partial f_{0p}/\partial\vec{p}_p}{m\Omega}d\vec{p}_p\right]\\&+\frac{i\nu_p}{n_{0p}^2\chi}\int\frac{p_{pi}f_{0p}d\vec{p}_p}{m\Omega}\left[\int\frac{m\omega-\vec{k}\cdot\vec{p}_p}{m\Omega}\frac{\partial f_{0p}}{\partial p_{pj}}d\vec{p}_p+\int\frac{p_{pj}}{m\Omega}\vec{k}\cdot\frac{\partial f_{0p}}{\partial\vec{p}_p}d\vec{p}_p\right].\end{aligned} \tag{6}$$

Here $\Omega=\omega-\vec{k}\cdot\vec{p}_p/m+i\nu_p$, $\chi=1-i(\nu_p/n_{0p})\int d\vec{p}_p f_{0p}/\Omega$, $\gamma_\alpha^*=(1+p_\alpha^2/m^2c^2)^{1/2}$ is the Lorentz factor and $\omega_\alpha=(4\pi n_{0\alpha}e^2/m)^{1/2}$ α-type electron plasma frequency, respectively. In deriving Eq. (6), we have assumed that the velocities of the background electrons are much less than the vacuum speed of light, so that the relativistic effect with them is ignored. Compared to the dielectric tensor expression presented before (e.g., Hao *et al.*, 2009*a*), the last term is associated with the correction of the Krook model as shown on the right-hand side of Eq. (1) for particle number conservation. The CFI mode is coupled to the Langmuir mode or ion acoustic mode due to the ε_{xz} and ε_{zx} on the right-hand side of Eq. (5). If the SCE is ignored, the dispersion relation can be simplified to

$$\varepsilon_{zz}-k^2c^2=0. \tag{7}$$

Thus, in the numerical calculation, we can turn on or turn off the SCE simply by including or ignoring ε_{xz} and ε_{zx}, respectively. Similarly, if we artificially set ν_p to be zero in Eq. (6), the collision is turned off so that we get the collisionless dispersion relation.

Generally, for the laser generated electron beam, a real unperturbed stationary state does not exist. However, the evolution of the beam parameters will not essentially affect the physics we are arguing. Thus, we can assume the beam satisfies the theoretical local equilibrium distribution function, i.e., the drift-Jiittner distribution (Wright *et al.*, 1975). Recently, it has been shown that such a distribution can well fit the beam distribution generated by laser-plasma interactions (Cottrill *et al.*, 2008). For convenience, here we use the saddle point expansion of the drift-Juttner distribution, i.e., the relativistic drift-Maxwellian distribution (Watson *et al.*, 1960) to model the beam electrons. This approximation is of good accuracy as long as the beam temperature is much smaller than the beam drift energy. The relativistic drift-Maxwellian distribution is

$$f_{0b}=\frac{n_{0b}}{2\pi m\gamma_b^2(T_{tb}T_{lb})^{1/2}}\exp\left[-\frac{p_x^2}{2m\gamma_bT_{tb}}-\frac{(p_z-P_{db})^2}{2m\gamma_b^3T_{lb}}\right], \tag{8}$$

where the Lorentz factor $\gamma_b=(1+P_{db}^2/m^2c^2)^{1/2}$, and T_{tb}, T_{lb}, and P_{db} correspond to trans-verse thermal temperature, longitudinal thermal temperature, and drift momentum of the beam electrons, respectively. The dense background plasma electron component is approximately treated using a non-relativistic drifting Maxwellian distribution as mentioned before. Substitute Eq. (8) into Eq. (6) and keep to the first order expansion of γ_α^*, we can get the dielectric tensor as follows:

$$\begin{aligned}\varepsilon_{zz}=\omega^2&-\frac{\omega_b^2}{\gamma_b^3}-\frac{\omega_b^2}{\gamma_b}\frac{p_{db}^2+m\gamma_b^3T_{lb}}{2m\gamma_bT_{tb}}Z'(\xi_b)\\&-\omega_p^2-\omega_p^2\frac{v_{dp}^2+v_{lp}^2}{2v_{tp}^2}Z'(\xi_p)\\&-i\omega_p^2\frac{\nu_p}{\sqrt{2}kv_{tp}}Z(\xi_p)+i\omega_p^2\frac{\nu_p}{\sqrt{2}kv_{tp}}\frac{v_{dp}^2}{2v_{tp}^2}\frac{Z(\xi_p)Z'(\xi_p)}{\chi(\xi_p)},\end{aligned} \tag{9}$$

$$\begin{aligned}\varepsilon_{xx}=\omega^2\Bigg[1&-\frac{\omega_b^2}{\gamma_b}\frac{Z'(\xi_b)}{2k^2T_{tb}/m}\\&-\omega_p^2\frac{\omega+i\nu_p}{\omega}\frac{Z'(\xi_p)}{2k^2v_{tp}^2}-i\frac{\omega_p^2}{k^2v_{tp}^2}\frac{\nu_p}{4\omega}\frac{Z'^2(\xi_p)}{\chi(\xi_p)}\Bigg],\end{aligned} \tag{10}$$

$$\begin{aligned}\varepsilon_{xz}=&-\frac{\omega_b^2}{\gamma_b}\frac{p_{db}}{\sqrt{2m\gamma_bT_{tb}}}\left(Z(\xi_b)+\frac{Z''(\xi_b)}{2}\right)\\&-\omega_p^2\frac{v_{dp}}{\sqrt{2}v_{tp}}\left(Z(\xi_p)+\frac{Z''(\xi_p)}{2}\right)\\&+i\omega_p^2\frac{v_{dp}}{2v_{tp}}\frac{\nu_p}{2kv_{tp}}\frac{Z'(\xi_p)}{\chi(\xi_p)},\end{aligned} \tag{11}$$

$$\begin{aligned}\varepsilon_{zx}=&-\frac{\omega_b^2}{\gamma_b}\frac{p_{db}}{\sqrt{2m\gamma_bT_{tb}}}\left(Z(\xi_b)+\frac{Z''(\xi_b)}{2}\right)\\&-\omega_p^2\frac{v_{dp}}{\sqrt{2}v_{tp}}\left(Z(\xi_p)+\frac{Z''(\xi_p)}{2}\right)\\&+i\omega_p^2\frac{v_{dp}}{v_{tp}}\frac{\nu_p}{kv_{tp}}\Bigg[-\frac{Z'(\xi_p)}{2}-\frac{\omega}{kv_{tp}}\frac{Z(\xi_p)Z'(\xi_p)}{2\sqrt{2}\chi(\xi_p)}\\&+\frac{Z(\xi_p)[Z(\xi_p)+Z''(\xi_p)/2+(i\nu_p/\sqrt{2}kv_{tp})Z'(\xi_p)]}{\chi(\xi_p)}\Bigg],\end{aligned} \tag{12}$$

https://doi.org/10.1017/S0263034613000803 Published online by Cambridge University Press

where $Z(\xi_\alpha) = \pi^{-1/2}\int_{-\infty}^{\infty} dt[e^{-t^2}/(t-\xi_\alpha)]$ is the plasma dispersion function (Fried *et al.*, 1968), $\zeta_\alpha = \sqrt{2T_{t\alpha}/\gamma_\alpha m}$, $\xi_b = \omega/k\zeta_b$, and $\xi_p = (\omega + i\nu_p)/k\zeta_p$, $\chi(\xi_p) = 1 + i\nu_p Z(\xi_p)/\sqrt{2}k\upsilon_{tp}$. In Eqs. (9)–(12), each of the last terms results from the inclusion of $\nu_\alpha(\delta n_\alpha/n_{0\alpha})f_{0\alpha}$ in the collision operator in Eq. (1). The numbers of primes on $Z(\xi_p)$ and $Z(\xi_b)$ denote the differentiation order. Since we usually encounter with an isotropic beam and an isotropic plasma, we denote $T_b = T_{tb} = T_{lb}$ and $T_p = T_{tp} = T_{lp}$. Although the ion motion is supposed to be important in the quasi-linear stage, we can get from Eq. (5) in the paper by Tzoufras *et al.* (2006) that the ion motion will not become important in the linear stage as long as $|\omega/k\upsilon_{tp}|^2 \gg 1/1836$. In our numerical results, we find this relation holds well except in the ultra dense region where $n_p > 500n_b$. However, in this region, collisional effects become important and the filamentation mode is fully decoupled from the ion-acoustic mode. The SCE then is rather weak and the ion motion can be ignored. Actually including the ion motion will not affect the main results of this paper, therefore, the ion motion is ignored in our linear theory in this work.

In order to compare with the particle-in-cell simulation results (Karmakar *et al.*, 2008) based on fluid distribution, we also present the dielectric tensor with the water-bag distribution functions. The distribution functions for beam and plasma electrons are described by (Bret *et al.*, 2005).

$$\begin{aligned} f_{0\alpha}(\vec{p}_\alpha) = {} & \frac{n_{0\alpha}}{4p_{t\alpha}p_{l\alpha}}[\Theta(p_x + p_{t\alpha}) - \Theta(p_x - p_{t\alpha})] \\ & \times [\Theta(p_z + p_{l\alpha} - p_{d\alpha}) \\ & - \Theta(p_z - p_{l\alpha} - p_{d\alpha})], \end{aligned} \tag{13}$$

where $\Theta(p)$ is the Heaviside function, $p_{t\alpha}$ and $p_{l\alpha}$ are the transverse and longitudinal momentum spread, respectively. For the dense background electron component, we can simply set $\gamma_p = 1$. Substitute Eq. (13) into Eq. (6) and keep to the first order expansion of γ_b^*, we can get the corresponding dielectric tensor components:

$$\begin{aligned} \varepsilon_{zz} = {} & \omega^2 - \frac{\omega_b^2}{\gamma_b^3} - \frac{\omega_b^2}{\gamma_b}\frac{k^2(p_{db}^2 + p_{lb}^2/3)}{m^2\gamma_b^2\omega^2 - k^2p_{tb}^2} \\ & - \omega_p^2 - \omega_p^2\frac{k^2(v_{dp}^2 + v_{lp}^2/3)}{\Delta} \\ & - i\omega_p^2\frac{\nu_p}{2k\upsilon_{tp}}\ln\varepsilon + i\omega_p^2\frac{\upsilon_{dp}^2}{2\upsilon_{tp}^2}\frac{\nu_p k\upsilon_{tp}}{\Delta}\frac{\ln\varepsilon}{\vartheta}, \end{aligned} \tag{14}$$

$$\begin{aligned} \varepsilon_{xx} = {} & \omega^2 - \omega_b^2\frac{\omega^2 m^2\gamma_b}{m^2\gamma_b^2\omega^2 - k^2p_{tb}^2} - \omega_p^2\frac{\omega(\omega + i\nu_p)}{\Delta} \\ & + i\omega_p^2\frac{\nu_p\omega}{\Delta}\frac{\vartheta'}{\vartheta}, \end{aligned} \tag{15}$$

$$\varepsilon_{zx} = -\omega_b^2\frac{kp_{db}m\omega}{m^2\gamma_b^2\omega^2 - k^2p_{tb}^2} - \omega_p^2\frac{k\upsilon_{dp}\omega}{\Delta} + i\omega_p^2\frac{\upsilon_{dp}}{2\upsilon_{tp}}\frac{\nu_p\omega}{\Delta}\frac{\ln\varepsilon}{\vartheta}, \tag{16}$$

$$\varepsilon_{xz} = -\omega_b^2\frac{kp_{db}m\omega}{m^2\gamma_b^2\omega^2 - k^2p_{tb}^2} - \omega_p^2\frac{k\upsilon_{dp}(\omega + i\nu_p)}{\Delta} + i\omega_p^2\frac{\nu_p\omega}{\Delta}\frac{\vartheta'}{\vartheta}. \tag{17}$$

where $\varepsilon = 1 - 2k\upsilon_{tp}/(\omega + i\nu_p + k\upsilon_{tp})$, $\vartheta = 1 + i(\nu_p/2k\upsilon_{tp})\ln(\varepsilon)$, $\vartheta' = 1 + [(\omega + i\nu_p)/2k\upsilon_{tp}]\ln\varepsilon$, and $\Delta = (\omega + i\nu_p)^2 - k^2\upsilon_{tp}^2$. Quite different from the results obtained with the drift-Maxwellian distribution function, there is no plasma dispersion function in the water-bag case. In fact, the dielectric tensors under these two distribution functions are approximately equal only in the fluid limit where $|\omega| \gg kp_{t\alpha}$. Note that in Eqs. (14)–(17), each of the last terms results from the inclusion of $\nu_\alpha(\delta n_\alpha/n_{0\alpha})f_{0\alpha}$ in the collision operator in Eq. (1).

3. GROWTH RATES OF THE INSTABILITIES

In this section, we study the collisional effects on the CFI with SCE. The rigorous current neutralization condition $n_b\upsilon_{db} + n_p\upsilon_{dp} = 0$ (Bell *et al.*, 1997) will be assumed from now on. Since the dielectric tensor is rather complex, it is very hard to get the analytic solutions to Eq. (5). Besides, the CFI is a purely growing instability so that the real part of the unstable solution is zero, i.e., $\mathrm{Re}(\omega) = 0$. Therefore, we will mainly focus on the numerical solution of the growth rates next. Figure 1a shows the maximum CFI growth rate versus the beam temperature obtained from Eq. (5) under typical parameters, where the most accurate Padé approximation Z_{53} (Martin *et al.*, 1980) for the plasma dispersion function is used (the other results in the following are obtained in the same way unless specially mentioned). We obtain the corresponding growth rates by turning on either the SCE or the collision, respectively. It is seen from Figure 1a that the SCE is negligible when the temperature difference between the beam and the background plasma is small. However, as the beam gets hotter, the temperature difference between the beam and the plasma becomes larger, therefore the SCE becomes stronger. It is seen from the dash-dotted line that when the SCE is not included, the maximum CFI growth rate is simply suppressed by half when the beam changes from cold to hot. However, when the SCE is included, the CFI is decreased more than one order of magnitude. Therefore, as we have discussed (Hao *et al.*, 2009*b*), it is the SCE, instead of the thermal spread (Silva *et al.*, 2002), that mainly suppresses the CFI. Although greatly attenuated, the CFI driven by the drift-anisotropy of the beam and plasma cannot be stabilized under drift-Maxwellian type distribution function (Cottrill *et al.*, 2008; Hao *et al.*, 2008; 2009*a*; Bret *et al.*, 2008). For comparison, we also plot the maximum growth rate obtained from the water-bag distribution only with transverse thermal spread (Bret *et al.*, 2005). The results (see Fig. 1c) are similar except that the CFI is fully stabilized when the beam temperature reaches 60 keV. However, the growth rate without the SCE is as large as 0.09, which is far from being stabilized. Therefore, it should be the SCE, rather than the thermal

https://doi.org/10.1017/S0263034613000803 Published online by Cambridge University Press

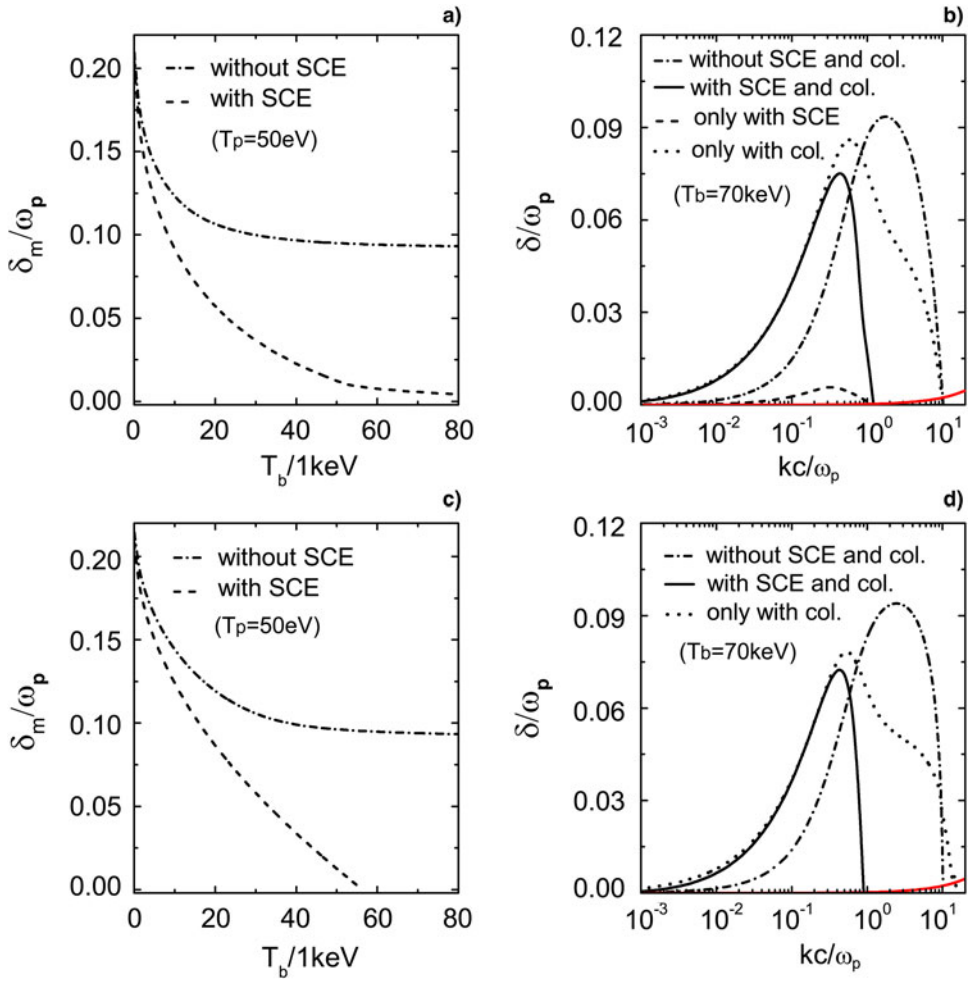


Fig. 1. (Color online) The maximum linear growth rate of the CFI *versus* the beam temperature (**a**) and (**c**), and the linear growth rate of the CFI *versus* the wave number k (**b**) and (**d**), respectively. The growth rate and the collision frequency are normalized by the background plasma frequency. The parameters are $n_p/n_b = 9$, $\upsilon_{bz} = 0.9$, $\nu_p/\omega_p = 0.15$, and $T_p = 50$ eV. T_b is normalized to keV for cases (a) and (c). Cases (a) and (b) are obtained with the drift-Maxwellian distribution, and (c) and (d) are obtained with the water-bag distribution, respectively. The red lines in (b) and (d) are given by $\delta = k\upsilon_{tp}/\sqrt{1836}$.

spread, which finally stabilizes the CFI in their corresponding simulation by Karmakar *et al.* (2008). The red lines in Figures 1b and 1d given by $\delta = k\upsilon_{tp}/\sqrt{1836}$ indicate that the effect of ion motion is neglectable in the linear stage.

Next, we consider the combination of SCE and collisional effects. It is argued that the SCE is significant only in the kinetic limit where the CFI is coupled to the ion acoustic mode (Hao *et al.*, 2009*b*). In the fluid limit, the SCE is coupled to the electron Langmuir mode. The thermal response time $(k\upsilon_\alpha)^{-1}$ under this case is much longer than the CFI growth time $|\omega|^{-1}$, so the coupling is weak and the SCE is inefficient. When collision is included, it changes ω into $\omega + i\nu_p$. If ν_p is much larger than $k\upsilon_{tp}$, $|\omega| \ll k\upsilon_{tp}$ can be changed into $|\omega + i\nu_p| \gg k\upsilon_{tp}$, thus the system is shifted from the kinetic domain into the hybrid or fluid domain, where the coupling between the CFI and the ion acoustic mode is weak. Therefore, collision can attenuate the SCE and enhance the CFI. This kind of mechanism is quite different from the resistive mechanism (Molvig, 1975, Hao *et al.*, 2009*a*), where collision appears to be resistive to the collective motion of the background electrons. For convenience, we denote it as the decoupling mechanism. Figure 1b shows the CFI growth rates with and without the SCE or collisional effects, respectively. It is seen from the dash- dotted line and the dotted line that when the SCE is neglected, the maximum collisional CFI growth rate is 0.07 while the maximum collisionless CFI growth rate is 0.09. Thus, the CFI is attenuated rather than enhanced by collision if the SCE is ignored. The result is similar to our previous investigation (Hao *et al.*, 2009*a*) that the CFI cannot be enhanced by collision due to resistive mechanism in the quasi-symmetric counter streaming region (when the plasma electron density is a few times of the beam electron density). In the case with SCE, the maximum collisionless growth rate is changed from 0.002 to 0.05 by collision. Therefore, the enhancement of the CFI at such condition should be due to attenuation of the

https://doi.org/10.1017/S0263034613000803 Published online by Cambridge University Press

SCE by collision, i.e., due to the decoupling mechanism. Figure 1d shows the CFI growth rates obtained from water-bag distribution function. The results are quite similar to those obtained with the drift-Maxwellian distribution except that the collisionless CFI with SCE is fully stabilized when the beam is hot. Although the CFI with SCE is stabilized when the beam temperature reaches 70 keV, we can see from the solid line in Figure 1d that it is regained if collision is present. Moreover, it is purely growing. Therefore, the regained CFI (or Weibel instability in Karmakar *et al.*, 2008) should be due to attenuation of the SCE by collision instead of the unstable negative-energy waves. The CFI is shifted to the long wavelength region by collision, resulting in larger filaments. Our present model with the SCE agrees quite well with the corresponding simulation results of Karmakar *et al.* (2008).

In order to further confirm the enhancement of the CFI of a quasi-symmetric counter streaming system is due to attenuation of the SCE by collision, we present a case where both the beam and the plasma are cold so that the SCE is weak. It is seen from the dashed lines in Figures 2a and 2b that the SCE is neglectable under such conditions. This time the decoupling mechanism is not significant. The maximum collisional CFI growth rates with and without the SCE are obviously smaller than the corresponding collisionless ones. That implies that collision attenuates the CFI under such conditions. This is in good agreement with our previous investigation (Hao *et al.*, 2009*a*) that collision cannot enhance the CFI for quasi-symmetric counter streaming system when SCE is neglectable. Note that our model cannot be applied to the symmetric counter-streaming configuration because we have modeled the plasma electrons to be non-relativistic.

From the results in Figures 1b and 1d, we can see that although the maximum collisional CFI growth rate with SCE can be improved compared with the collisionless case with SCE, it is still decreased compared with the collisionless CFI without SCE. This is an important difference between the decoupling mechanism and the resistive mechanism. In the resistive mechanism, the collisional growth rate can be much larger than the corresponding collision- less one without SCE. Next, we shall include both the SCE and the collisional effects and apply the present theory to the parameter regime relevant to laser-solid interaction and FIS.

Figures 3a and 3b depict the maximum CFI growth rate relevant to FIS as a function of the background plasma density for $T_p = 250$ eV and 1 keV, correspondingly. In the collisionless case, the SCE is more important in the 250 eV case since the temperature difference between the beam and the background plasma is larger. It is seen from Figure 3a that the CFI is suppressed by several factors of magnitude by the SCE in the region $n_p < 100n_b$. As the plasma density gets larger, the SCE becomes weaker. When collision is included, it acts to attenuates the SCE. We have argued in previous investigations that collisional effects tend to attenuate the CFI for quasi-symmetric counter streaming while enhancing it for extremely asymmetric counter streaming if the SCE is ignored (Hao *et al.*, 2008; Hao *et al.*, 2009*a*). However, when SCE is taken into account, it is seen from Figures 3a and 3b that the maximum collisional CFI growth rates with SCE are always enhanced compared with the corresponding collisionless ones for asymmetric counter streaming cases. In the low plasma density region, the enhanced CFI with SCE is due to attenuation of the SCE by collision, i.e., due to the decoupling mechanism. In the dense region, the CFI is enhanced due to both the decoupling mechanism and the usual resistive mechanism, and the later one usually plays the dominant role. Although the collisional CFI with SCE is always enhanced compared with the collisionless CFI with SCE, it is still attenuated compared with the

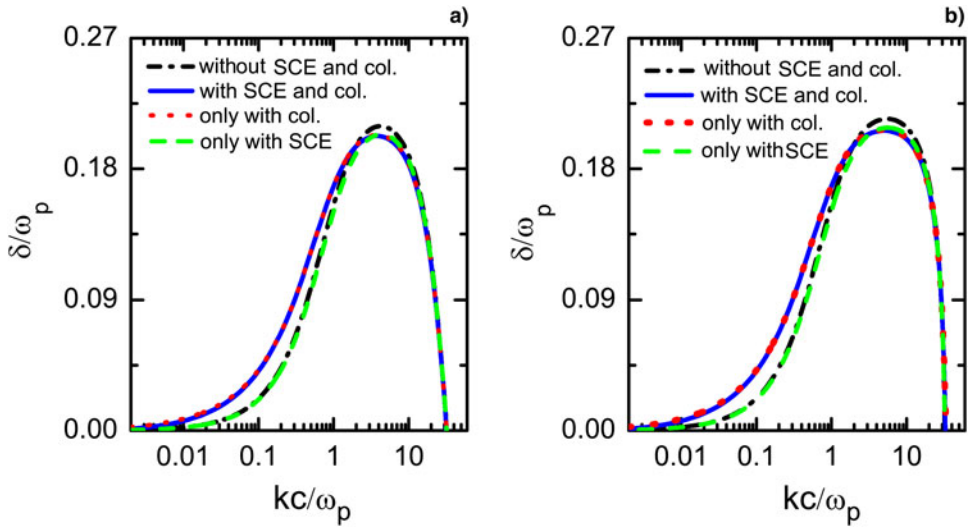


Fig. 2. (Color online) The linear growth rate of the CFI *versus* the wave number k obtained by solving Eq. (5). The growth rate and the collision frequency are normalized by the background plasma frequency. $T_b = 50$ eV, and the other parameters are the same as those in Figure 1b. Cases (**a**) and (**b**) are obtained with the drift-Maxwellian distribution and the water-bag distribution, respectively.

https://doi.org/10.1017/S0263034613000803 Published online by Cambridge University Press

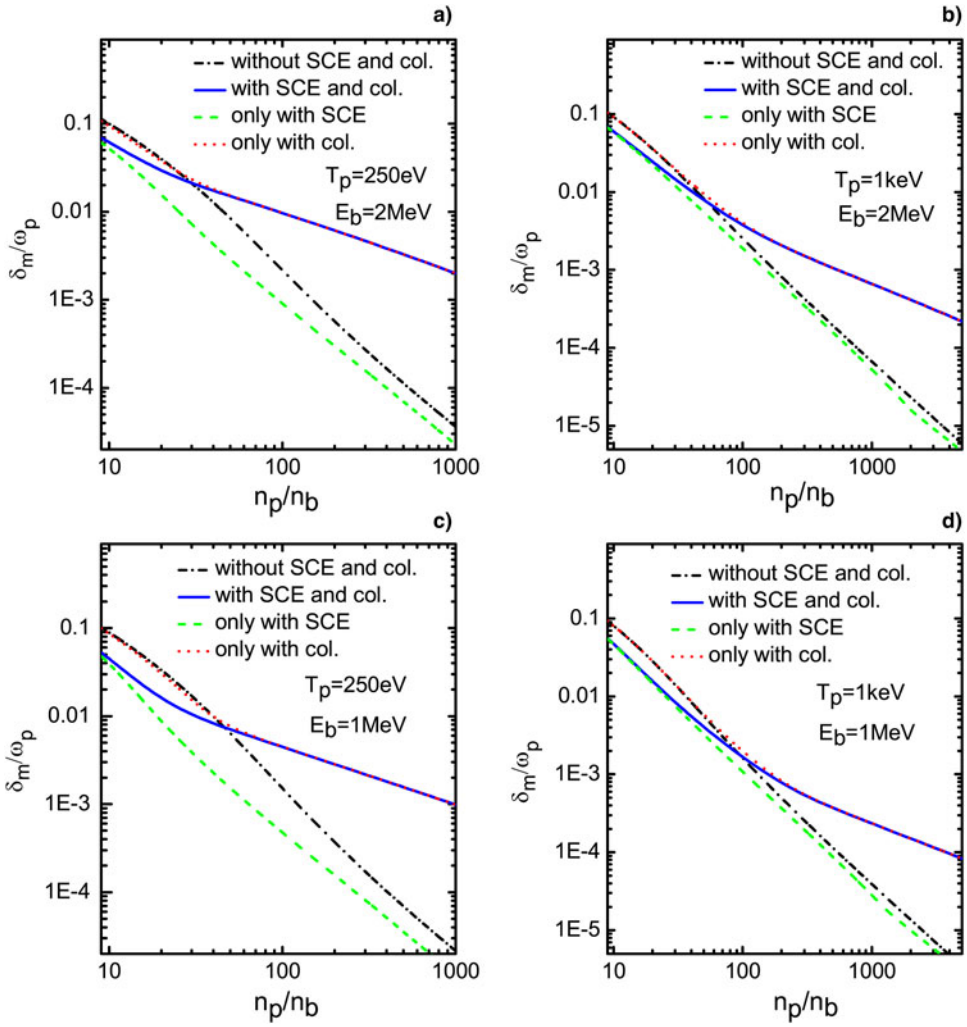


Fig. 3. (Color online) The maximum linear growth rate of the CFI *versus* the background plasma density n_p obtained by solving Eq. (5). The other parameters for cases (**a**) and (**b**) are given by $n_b = 10^{22}\text{cm}^{-3}$, $\upsilon_{db} = 0.979$ ($E_b = 2$ MeV), and $T_b = 30$ keV, and those for cases (**c**) and (**d**) are given by $n_b = 10^{21}\text{cm}^{-3}$, $\upsilon_{db} = 0.941$ ($E_b = 1$ MeV), and $T_b = 30$ keV, where E_b is the kinetic energy of the beam electrons.

collisionless CFI without the SCE in the quasi-symmetric region where $n_p < 50n_b$. This is in good agreement with our above discussion that the decoupling mechanism cannot increase the growth rate beyond the collisionless one without SCE.

In the ultra-dense region where $n_p > 100n_b$, it is seen both from Figures 3a and 3b that the SCE is fully suppressed by collision so that the maximum collisional CFI growth rates with and without SCE are equal. The SCE at this moment are neglectable in the collisional case. Therefore, our previous results (Hao *et al.*, 2009*a*) obtained in the ultradense region without considering the SCE are a good approximation. For comparison, we also plot in Figures 3c and 3d the maximum growth rates of the CFI under parameters of the former paper (Hao *et al.*, 2009*a*). It is seen that the main results are quite similar to those in Figures 2a and 2c in that paper, respectively. Since the CFI growth rate is one or two orders of magnitude larger than the beam electron collision frequency in the dense core, the incoming fast electron beam may potentially break into filaments even in the dense region at the linear stage. More over, the filamentation induced kinetic anomalous target heating might be important for the electron energy deposition (Honda *et al.*, 2000; Sentoku *et al.*, 2003). For laser-solid interactions, since the background plasma usually has a very low temperature, the SCE is much more significant. It is expected from Figure 1 that the decoupling mechanism will play an important role for the development of the CFI.

4. SUMMARY

We have investigated theoretically the collisional effects on the relativistic CFI with SCE taking into account. The different roles which collisions play on the CFI with and without SCE are identified. In the case without SCE, the CFI is affected by collision through resistive mechanism, where it is

https://doi.org/10.1017/S0263034613000803 Published online by Cambridge University Press

attenuated in the quasi-symmetric counter streaming configuration but enhanced in the extremely asymmetric counter streaming configuration. In the case with SCE, the CFI is affected by collision through both the resistive mechanism and the decoupling mechanism, where it might be also enhanced in the quasi-symmetric counter streaming configuration through decoupling mechanism. In particular, we find the regained CFI found in the two-dimensional numerical simulation (Karmakar *et al.*, 2008) may be due to attenuation of SCE by collision, i.e., due to the decoupling mechanism, rather than the unstable negative-energy magneto sound waves driven by collisions in the background plasma.

The above theory is then applied to laser-solid interaction and FIS where both the collisional effects and SCE are important for the kinetic collective instability. It is found in a hot-beam warm-plasma system that the maximum CFI with SCE is always enhanced by collisions compared with the collisionless CFI with SCE no matter how large the background plasma density is. As the plasma density gets higher, the CFI growth rate is enhanced more than one order of magnitude, which indicates that the incoming fast electron beam inclines to break into small filaments even in the dense region. This results in not only the generation of quasi-static magnetic fields but also potentially anomalous target core heating.

ACKNOWLEDGMENTS

This work is supported in part by the National Basic Research Program of China (Grant No. 2013CBA01504) and the National Science Foundation of China (Grant No. 11121504, 11075105, and 11220101002).

REFERENCES

Baton, S.D., Batani, D., Manclossi, M., Morace, A., Piazza, D., Benuzzi-Mounaix, A., Koenig, M., Guillou, P., Loupias, B., Fuchs, J., Amiranoff, F., Gloahec, M.R.L., Popescu, H., Rousseaux, C., Borhesi, M., Cecchetti, C., Kodama, R., Norimatsu, T., Nakatsutsumi, M. & Aglitskiy, Y. (2005). Recent experiments on electron transport in high-intensity laser matter interaction. *Plasma Phys. Contr. Fusion* **47**, B777–B790.

Bell, A.R., Davies, J.R., Guerin, S. & Ruhl, H. (1997). Fast-electron transport in high-intensity short-pulse laser-solid experiments. *Plasma Phys. Contr. Fusion* **39**, 653–660.

Bhatnagar, P.L., Gross, E.P. & Krook, M. (1954). A model for collision processes in gases. I. Small amplitude processes in charged and neutral one-component systems. *Phys. Rev.* **94**, 511–525.

Bludman, S.A., Watson, K.M. & Rosenbluth, M.N. (1960). Statistical mechanics of relativistic streams. II. *Phys. Fluids* **3**, 747–757.

Breizman, B.N. & Ryutov, D.D. (1974). Powerful relativistic electron beams in a plasma and in a vacuum. *Nucl. Fusion* **14**, 873–907.

Bret, A., Firpo, M.C. & Deutsch, C. (2005). Electromagnetic instabilities for relativistic beam-plasma interaction in whole k space: Nonrelativistic beam and plasma temperature effects. *Phys. Rev. E* **72**, 016403.

Bret, A., Firpo, M.-C. & Deutsch, C. (2006). Between two stream and filamentation instabilities: Temperature and collisions effects. *Laser Part. Beams* **24**, 27–33.

Bret, A., Gremillet, L. & Dellido, J.C. (2007). How really transverse is the filamentation instability? *Phys. Plasmas* **14**, 032103.

Bret, A., Gremillet, L., Benisti, D. & Lefebvre, E. (2008). Exact relativistic kinetic theory of an electron-beam-plasma system: hierarchy of the competing modes in the system-parameter space. *Phys. Rev. Lett.* **100**, 205008.

Bret, A., Fernandez, F.J.M. & Anfray, J.M. (2009). Unstable spectrum of a relativistic electron beam interacting with a quantum collisional plasma: application to the fast ignition scenario. *Plasma Phys. Contr. Fusion* **51**, 075011.

Bret, A. (2010). Collisional and collisionless beam plasma instabilities. *Laser Part. Beams* **28**, 491–495.

Califano, F., Pegoraro, F., Bulanov, S.V. & Mangeney, A. (1998). Kinetic saturation of the Weibel instability in a collisionless plasma. *Phys. Rev. E* **57**, 7048–7059.

Chrisman, B., Sentoku, Y. & Kemp, J. (2008). Intensity scaling of hot electron energy coupling in cone-guided fast ignition. *Phys. Plasmas* **15**, 056309.

Cottrill, L.A., Langdon, A.B., Lansinki, B.F., Lund, S.M., Molvig, K., Tabak, M., Town, R.P.J. & Williams, E.A. (2008). Kinetic and collisional effects on the linear evolution of fast ignition relevant beam instabilities. *Phys. Plasmas* **15**, 082108.

Deutsch, C. & Didelez, J.-P. (2011). Inertial confinement fusion fast ignition with ultra-relativistic electron beams. *Laser Part. Beams* **29**, 39–44.

Duclousa, R., Morreeuw, J.P., Tikhonchuk, V.T. & Dubroca, B. (2008). Reduced multi-scale kinetic models for the relativistic electron transport in solid targets: Effects related to secondary electrons. *Laser Part. Beams* **28**, 165–177.

Fonseca, R.A. & Silva, L.O. (2003). Three-dimensional Weibel instability in astrophysical scenarios. *Phys. Plasmas* **10**, 1979–1984.

Fried, B.D., Hedrick, C.L. & McCune, J. (1968). Two-pole approximation for the plasma dispersion function. *Phys. Fluids* **11**, 249–252.

Gremillet, L., Bonnaud, G. & Amiranoff, F. (2002). Filamented transport of laser-generated relativistic electrons penetrating a solid target. *Phys. Plasmas* **9**, 941–948.

Hao, B., Sheng, Z.M. & Zhang, J. (2008). Kinetic theory on the current-filamentation instability in collisional plasmas. *Phys. Plasmas* **15**, 082112.

Hao, B., Sheng, Z.M., Ren, C. & Zhang, J. (2009*a*). Relativistic collisional current-filamentation instability and two-stream instability in dense plasma. *Phys. Rev. E* **79**, 046409.

Hao, B., Ding, W.J., Sheng, Z.M., Ren, C. & Zhang, J. (2009*b*). Plasma thermal effect on the relativistic current-filamentation and two-stream instabilities in a hot-beam warm-plasma system. *Phys. Rev. E* **80**, 066402.

Hao, B., Ding, W.J., Sheng, Z.M., Ren, C., Kong, X., Mu, J. & Zhang, J. (2012). Collisional effects on the oblique instability in relativistic beam-plasma interactions. *Phys. Plasmas* **19**, 072709.

Hill, J.M., Key, M.H., Hatchett, S.P. & Freeman, R.R. (2005). Beam-Weibel filamentation instability in near-term and fast-ignition experiments. *Phys. Plasmas* **12**, 082304.

https://doi.org/10.1017/S0263034613000803 Published online by Cambridge University Press

Honda, M., Meyer-ter-Vehn, J. & Pukhov, A. (2000). Collective stopping and ion heating in relativistic-electron-beam transport for fast ignition. *Phys. Rev. Lett.* **85**, 2128–2131.

Honda, M. (2004). Eigenmodes and growth rates of relativistic current filamentation instability in a collisional plasma. *Phys. Rev. E* **69**, 016401.

Honrubia, J.J. & Meyer-ter-Vehn, J. (2008). Fast ignition of fusion targets by laser-driven electrons. *Plasma Phys. Contr. Fusion* **51**, 014008.

Jung, R., Osterholz, J., Lowenbruck, K., Kiselev, S., Pretzler, G., Pukhov, A., Willi, O., Kar, S., Borghesi, M., Nazarov, W., Karsch, S., Claeke, R. & Neely, D. (2009). Study of electron-beam propagation through preionized dense foam plasmas. *Phys. Rev. Lett.* **94**, 195001.

Karmakar, A., Kumar, N., Shvets, G., Polomarov, O. & Pukhov, A. (2008). Collision-driven negative-energy waves and the Weibel instability of a relativistic electron beam in a quasineutral plasma. *Phys. Rev. Lett.* **101**, 255001.

Kodama, R., Norreys, P.A., Mima, K., Dangor, A.E., Evans, R.G., Fujita, H., Kitagawa, Y., Krushelnick, K., Miyakoshi, T., Miyanaga, N., Norimatsu, T., Rose, S.J., Shozaki, T., Shigemori, K., Sunahara, A., Tampo, M., Tanakaka, K.A., Toyama, Y., Yamanaka, T. & Zepf, M. (2001). Fast heating of ultrahigh-density plasma as a step towards laser fusion ignition. *Nature* **412**, 798–802.

Kong, X., Park, J., Ren, C., Sheng, Z.M. & Tong, J.W. (2009). Evolution of a relativistic electron beam-plasma return current system. *Phys. Plasmas* **16**, 032107.

Lalousis, P., Foldes, I.B. & Hora, H. (2012). Ultrahigh acceleration of plasma by picosecond terawatt laser pulses for fast ignition of fusion. *Laser Part. Beams* **30**, 233–242.

Lee, H. & Thode, L.E. (1983). Electromagnetic two-stream and filamentation instabilities for a relativistic beam-plasma system. *Phys. Fluids* **26**, 2707–2716.

Li, Y.T., Li, C., Zhou, M.L., Wang, W.M., Du, F., Ding, W.J., Lin, X.X., Liu, F., Sheng, Z.M., Peng, X.Y., Chen, L.M., Ma, J.L., Lu, X., Wang, Z.H., Wei, Z.Y. & Zhang, J. (2012). Strong terahertz radiation from relativistic laser interaction with solid density plasmas. *Appl. Phys. Lett.* **100**, 254101.

Lin, X.X., Li, Y.T., Liu, B.C., Liu, F., Du, F., Wang, S.J., Chen, L.M., Zhang, L., Liu, X., Liu, X.L., Wang, Z.H., Ma, J.L., Lu, X., Dong, Q.L., Wang, W.M., Sheng, Z.M., Wei, Z.Y. & Zhang, J. (2012). Directional transport of fast electrons at the front target surface irradiated by intense femtosecond laser pulses with preformed plasma. *Laser Part. Beams* **30**, 39–43.

Martin, P., Donoso, G. & Cristi, J.Z. (1980). A modified asymptotic Pad method. Application to multipole approximation for the plasma dispersion function Z. *J. Math. Phys.* **21**, 280–285.

Medvedev, M.V. & Loeb, A. (1999). Generation of magnetic fields in the relativistic shock of gamma-ray burst sources. *Astrophys. J.* **526**, 697–706.

Meyer-ter-Vehn, J., Honrubia, J., Geissler, M., Karsch, S., Krausz, F., Tsakiris, G. & Witte, K. (2005). On electron transport in fast ignition research and the use of few-cycle PW-range laser pulses. *Plasma Phys. Contr. Fusion* **47**, B807–B813.

Mondal, S., Narayanan, V., Ding, W.J., Lad, A.D., Hao, B., Ahmad, S., Wang, W.M., Sheng, Z.M., Sengupta, S., Kaw, P.K., Das, A. & Kumar, G.R. (2012). Direct observation of turbulent magnetic fields in hot, dense laser produced plasmas. *Proc. Nat. Acad. Sci.* **109**, 8011–8015.

Molvig, K. (1975). Filamentary instability of a relativistic electron beam. *Phys. Rev. Lett.* **35**, 1504–1507.

Okada, T. & Niu, K. (1980). Effect of collisions on the relativistic electromagnetic instability. *J. Plasma Phys.* **24**, 483–488.

Pegoraro, F., Bulanov, S.V., Califano, F. & Lontano, M. (1996). Nonlinear development of the weibel instability and magnetic field generation in collisionless plasmas. *Phys. Scr.* **T63**, 262–265.

Pukhov, A. & Meyer-ter-Vehn, J. (1997). Laser hole boring into overdense plasma and relativistic electron currents for fast ignition of ICF targets. *Phys. Rev. Lett.* **79**, 2686–2689.

Roth, M., Brambrink, E., Audebert, P., Blazevic, A., Clarke, R., Cobble, J., Cowan, T.E., Fernandez, J., Fuchs, J., Geissel, M., Habs, D., Hegelich, M., Karsch, S., Ledingham, K., Neely, D., Ruhl, H., Schlegel, T. & Schreiber, J. (2005). Laser accelerated ions and electron transport in ultra-intense laser matter interaction. *Laser Part. Beams* **23**, 95–100.

Sakagami, H., Okada, K., Kaseda, Y., Taguchi, T. & Johzaki, T. (2012). Collisional effects on fast electron generation and transport in fast ignition. *Laser Part. Beams* **30**, 243–248.

Sentoku, Y., Mima, K., Kojima, S. & Ruhl, H. (2000). Magnetic instability by the relativistic laser pulses in overdense plasmas. *Phys. Plasmas* **7**, 689–695.

Sentoku, Y., Mima, K., Kaw, P. & Nishikawa, K. (2003). Anomalous resistivity resulting from MeV-electron transport in overdense plasma. *Phys. Rev. Lett.* **90**, 155001.

Silva, L.O., Fonseca, R.A., Tonge, J.W., Mori, W.B. & Dawson, J.M. (2002). On the role of the purely transverse Weibel instability in fast ignitor scenarios. *Phys. Plasmas* **9**, 2458–2461.

Startsev, E.A., Davidson, R.C. & Qin, H. (2002). Nonlinear delta-f simulation studies of intense charged particle beams with large temperature anisotropy. *Laser Part. Beams* **20**, 585–588.

Stockem, A., Dieckmann, M.E. & Schlickeiser, R. (2009). PIC simulations of the thermal anisotropy-driven Weibel instability: field growth and phase space evolution upon saturation. *Plasma Phys. Contr. Fusion* **51**, 075014.

Storm, M., Solodov, A.A., Myatt, J.F., Meyerhofer, D.D., Stoeckl, C., Mileham, C., Betti, R., Nilson, P.M., Sangster, T.C., Theobald, W. & Guo, C. (2009). High-current, relativistic electron-beam transport in metals and the role of magnetic collimation. *Phys. Rev. Lett.* **102**, 235004.

Tabak, M., Hammer, J., Glinsky, M.E., Kruer, W.L., Wilks, S.C., Woodworth, J., Campbell, E.M., Perry, M.D. & Mason, R.J. (1994). Ignition and high gain with ultrapowerful lasers. *Phys. Plasmas* **1**, 1626–1634.

Takabe, H., Kato, T.N., Sakawa, Y., Kuramitsu, Y., Morita, T., Kadono, T., Shigemori, K., Otani, K., Nagatomo, H., Norimatsu, T., Dono, S., Endo, T., Miyanishi, K., Kimura, T., Shiroshita, A., Ozaki, N., Kodama, R., Fujioka, S., Nishimura, H., Salzman, D., Loupias, B., Gregory, C., Koenig, M., Waugh, J.N., Woolsey, N.C., Kato, D., Li, Y.T., Dong, Q.L., Wang, S.J., Zhang, Y., Zhao, J., Wang, F.L., Wei, H.F., Shi, J.R., Zhao, G., Zhang, J.Y., Wen, T.S., Zhang, W.H., Hu, X., Liu, S.Y., Ding, Y.K., Zhang, L., Tang, Y.J., Zhang, B.H., Zheng, Z.J., Sheng, Z.M. & Zhang, J. (2008). High-Mach number collisionless shock and photo-ionized non-LTE plasma for

https://doi.org/10.1017/S0263034613000803 Published online by Cambridge University Press

laboratory astrophysics with intense lasers. *Plasma Phys. Contr. Fusion* **50**, 124057.

Tatarakis, M., Beg, F.N., Clark, E.L., Dangor, A.E., Edwards, R.D., Evans, R.G., Goldsack, T.J., Ledingham, K.W.D., Norreys, P.A., Sinclair, M.A., Wei, M.S., Zepf, M. & Krushelnick, K. (2003). Propagation instabilities of high-intensity laser-produced electron beams. *Phys. Rev. Lett.* **90**, 175001.

Tzoufras, M., Ren, C., Tsung, F.S., Tonge, J.W., Mori, W.B., Fiore, M., Fonseca, R.A. & Silva, L.O. (2006). Space-charge effects in the current-filamentation or Weibel instability. *Phys. Rev. Lett.* **96**, 105002.

Watson, K.M., Bludman, S.A. & Rosenbluth, M.N. (1960). Statistical mechanics of relativistic streams. I. *Phys. Fluids* **3**, 741–747.

Weibel, E.S. (1959). Spontaneously growing transverse waves in a plasma due to an anisotropic velocity distribution. *Phys. Rev. Lett.* **2**, 83–84.

Wright, T.P. & Hadley, G.R. (1975). Relativistic distribution functions and applications to electron beams. *Phys. Rev. A* **12**, 686–697.

Zhou, C.T., Cai, T.X., Zhang, W.Y. & He, X.T. (2012). Effect of plasma material on intense laser-driven beam electrons in solid foils. *Laser Part. Beams* **30**, 111–116.

https://doi.org/10.1017/S0263034613000803 Published online by Cambridge University Press